

## INVESTIGATION OF $\text{Ar}^+$ IONS SCATTERING FROM THE SURFACE OF $\text{CdTe}(001) \langle 110 \rangle$ AT THE GLANCING INCIDENCE

Sh.R. Sadullaev<sup>a\*</sup>, Uchkun O. Kutliev<sup>a</sup>, A.Yu. Saidova<sup>a</sup>, G.O. Jumanazarov<sup>a</sup>, R.R. Ruzmetov<sup>b</sup>

<sup>a</sup>Urgench State University named after Abu Raykhan Beruni, Department of Physics,  
Khamid Olimjan street.14, Urgench 220100, Uzbekistan

<sup>b</sup>Military-academically lyceum named after Jaloliddin Manguberdi, Urgench 220100, Uzbekistan

\*Corresponding Author e-mail: [sadullayev.sh.r@gmail.com](mailto:sadullayev.sh.r@gmail.com)

Received January 27, 2025; revised April 3, 2025; accepted April 28, 2025

This article presents the results of ion scattering from the surface of a thin film of  $\text{CdTe}(001) \langle 110 \rangle$ , obtained using ion stripping spectroscopy. The trajectories of scattered  $\text{Ar}^+$  ions were obtained and analyzed, with an initial energy of 1 keV and at angles of incidence  $\psi = 3^\circ$  and  $7^\circ$ . It is shown that the trajectories of scattered ions from the surface atomic row, from the wall of the semichannel and from the bottom of the semichannel differ from each other. The first trajectories of scattered ions from a surface semichannel consisting of five Cd and Te atoms arranged layer-by-layer in two layers were obtained. The shapes of these three types of trajectories are discussed and the energies, scattering coefficients, and inelastic energy losses of the scattered ions are calculated. It is shown that the energy values, scattering coefficient and inelastic energy losses of scattered ions from surface atomic rows differ little from each other. For ions scattered from the wall of the semichannel and from the bottom of the semichannel, the values of these parameters lie in the range.

**Keywords:** Computer simulation; Ion scattering; Semichannel; Trajectory scattered ions

**PACS:** 34.35.+a, 68.49.Sf, 79.20.Rf

### INTRODUCTIONS

The use of ion probing is one of many available methods for studying surfaces. And it provides a wide range of energies and the ability to obtain information about composition and structure, using many equipment. One of the methods is the ion scattering spectroscopy method. The range of energies used in ion scattering is usually divided into three parts. Low energy ion scattering (LEIS, energies 500–10 keV), intermediate energy ion scattering (MEIS, 10–600 keV) and high energy ion scattering (HEIS,  $>1$  MeV), these definitions have never been rigid. Ion scattering research did not become widespread until the early fifties of the last century and was concentrated mainly in the HEIS energy region. These studies tested the two-body collision model and found it to be applicable and ultimately led to the development of Rutherford backscattering (RBS). Lower energies were carried out in the late fifties of the last century [1–4], which found that the maximum energy of scattered ions corresponds to the prediction of the classical model of successive collisions. This was followed by the development of this line of research, which applied this method to the analysis of the elemental composition in the outermost monolayer, this led to a rapid increase in the number of studies on ion scattering. There is currently active research into many aspects of ion scattering, such as ion neutralization and the effects of different work functions or the determination of the universal scattering potential [5–9], and there is considerable interest in its application to the determination of surface structures.

It is known that  $\text{CdTe}$  thin films belong to  $\text{A}^{\text{II}}\text{B}^{\text{VI}}$  semiconductor compounds, which. And also,  $\text{CdTe}$ -based solar cells attract attention because  $\text{CdTe}$  is characterized by direct energy band gap  $E_g$  and high absorption coefficient, which makes  $\text{CdTe}$  an excellent light-absorbing layer of solar cells. Therefore, obtaining and studying  $\text{CdTe}$  films is of great interest. And this work presents the results of studying the  $\text{CdTe}$  surface using the ion scattering spectroscopy method.

### RESEARCH METHOD AND RESULTS

In the region of medium energies, the trajectories of colliding particles are determined to a first approximation by the forces of elastic interaction of atoms. These forces arise from the Coulomb forces of interaction between nuclei and electron atoms and, therefore, act at any distance between the interacting particles. Consequently, to calculate the trajectory of an incident ion, it is necessary to consider its interaction in the crystal lattice with all atoms simultaneously, which is very difficult. But at not very low energies, ion – atom collisions can be considered as isolated pair collisions of particles. Confirmation that the lattice atoms are free during collisions, i.e. behave like atoms of a dense gas, are the results of a study of the interaction time and energy of colliding particles [10–14].

In the pair collision approximation model, it appears that a particle of mass  $M_1$  with atomic number  $Z_1$ , with speed  $v_0$  (and kinetic energy  $E_0$ ), collides with a stationary target atom of mass  $M_2$  and atomic number  $Z_2$ . As a result of interaction, the incident particle is scattered in the laboratory coordinate system at an angle  $\theta_{\text{ofl}}$  relative to the direction of its initial motion. In this case, the target atom as a result of the collision begins to move in a direction that makes an angle of  $\theta_2$  with

the initial direction of the incident particle. Applying the law of conservation of energy and momentum to an elementary act of interaction, we obtain for energy  $E_1$  scattered particle the following relationship:

$$E_1 = (1 + \mu)^{-2} E_0 (\cos \theta_1 \pm \sqrt{(f\mu)^2 - \sin^2 \theta_1})^2$$

For the particles, interaction description the Ziegler – Biersack – Littmark (ZBL) potential [15] with regard to the time integral was used. The ZBL approximation for the screening function in the Thomas – Fermi potential takes into account the exchange and correlation energies and the so-called “universal” potential, obtained in this way shows good agreement with experiment over a wide range of interatomic separations. To estimate the in elastic energy loss in an elementary collision event, we used the Firsov formula modified by Kishinevsky [16].

In Fig.1. a semichannel formed on the surface of CdTe(001) <110> and a diagram of ion scattering from this semichannel are presented. The depth and width of the semichannel are 2.28Å and 4.64Å, respectively. Here  $\psi$  is the incidence angle,  $\varphi$  is the azimuthal scattering angle, and  $\sigma$  is the polar scattering angle. In our calculations, the aiming point is a is divided into coordinates I and J, which presented on the Fig.1. It should be noted that with increasing coordinates I we cover the entire width of the semichannel Due to the symmetry of the semichannel, it is enough for us to use I/2 in our calculations, since we can symmetrically cover the entire width of the semichannel. Kinematics of the elementary act of collision of two particles within the framework of classical mechanics, making it possible to establish a connection between the characteristics of particles before and after the collision. Velocity (energy) of an incident ion with mass  $m_1$  after the collision were determined by the laws of conservation of momentum and energy.

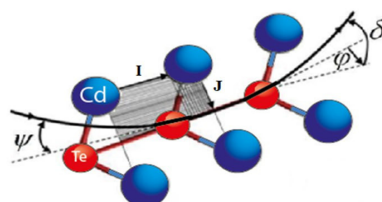


**Figure 1.** Semichannel and ion scattering scheme

In Fig. 2. a semichannel on the CdTe(001) <110> surface and the trajectories of scattered Ar<sup>+</sup> ions after bombardment at grazing angles are presented. In the calculations, the angle of incidence was  $\psi=3^\circ$  and  $7^\circ$ , and the initial energy was 1 keV. In Fig. 2. the trajectories of scattered ions at  $\psi=3^\circ$  are presented. At first glance, one can see different trajectories of the scattered ion. Some of them end inside the semichannel and this shows that ions are implanted inside the crystal. It should be noted that reflections from the surface atom and the bottom atom of the semichannel are clearly visible. To understand the whole picture of the ion scattering process, we divide these trajectories into 3 groups. The first are the trajectories of scattered ions from the surface atomic row (1), second – from the wall of the surface atomic semichannel (2), and the third – from the bottom of the semichannel (3). The figure also shows that in these three areas there are stepped dense areas (7 pieces). Calculations have shown that dense areas are formed due to parallel trajectories, i.e., the trajectory incident and reflected particles do not diverge. Such trajectories can be observed in the three groups mentioned above. These three trajectory groups are shown separately in Fig. 3.

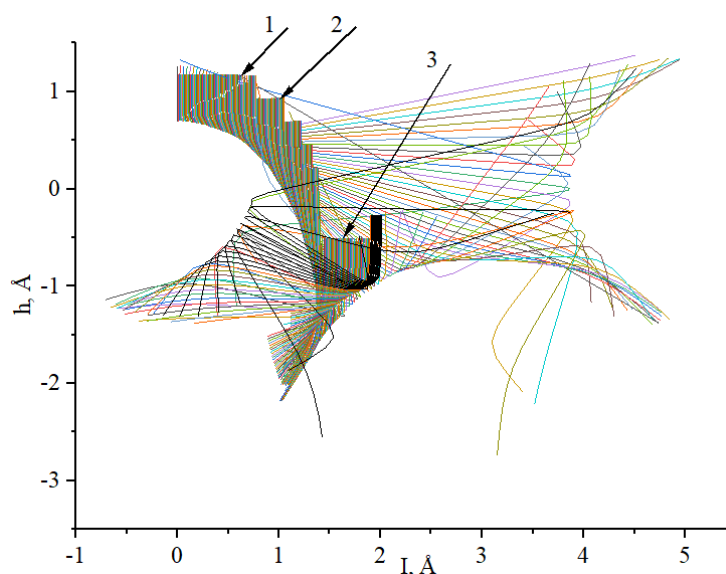


**Figure 2.** Trajectories of scattered Ar<sup>+</sup> ions from the surface of CdTe(001) <110> at  $\psi=3^\circ$  and  $E_0=1$  keV.

Fig. 3a shows the trajectories of ions belonging to the first group, i.e. trajectories of ions scattered from the surface atomic row. It can be seen that at initial values of  $I$ , trajectories are observed whose projections of the incident and scattered parts are almost parallel. The parallelism is especially clearly visible when  $I = 1$ . And starting from  $I = 2$ , deviations from the original direction occur. It can be seen that further increases in the value of  $I$  lead to deviations from the initial direction towards the center of the semichannel. This is explained by the fact that as the value of  $I$  increases, the incident ions begin to collide with the edges of the surface atom and change their trajectories towards the center of the semichannel. Early calculations showed that the ions scattered from the surface atomic row have an energy of 991 eV, the scattering coefficient is -7, and the inelastic energy loss is -8 eV. This shows that the bombarding ions will lose about 10% of the initial energy at a grazing angle  $\psi=3^\circ$ .

In Fig. 3b. some trajectories belonging to group 2 are presented. These trajectories have different shapes. It can be seen that these trajectories also have trajectories in which the incident and reflected parts are similar. These trajectories are formed by scattering of ions from the surface atomic row and the bottom of the semichannel. Therefore, the projection trajectories are curves. And also, trajectories were observed that were not similar to the incident reflected part. This shows that the ion is first scattered from the surface atomic row, and then scattered from the atom located at the bottom of the semichannel and leaves this semichannel. There is also a trajectory similar to a loop (red trajectory). This trajectory is formed due to the scattering of the ion from the surface atomic row, then from the bottom of the hemichannel, and then again from the surface atomic row before exiting the hemichannel. Early calculations showed that ions scattered from the surface atomic row have an energy in the range of 968-980 eV, a scattering coefficient in the range of -14-30, and inelastic energy losses -15-29 eV.

In Fig. 3c. The trajectory of scattered ions belonging to group 3 is presented. It can be seen that the trajectory of the ions has an almost parallel shape to each other. And these ions remained (implanted) inside the crystal and before that were first scattered from the bottom of the semichannel, and then from the surface atom. They have the same physical parameters (energy 981-987 eV, dissipation coefficient -14-16, inelastic energy losses -12-17 eV).

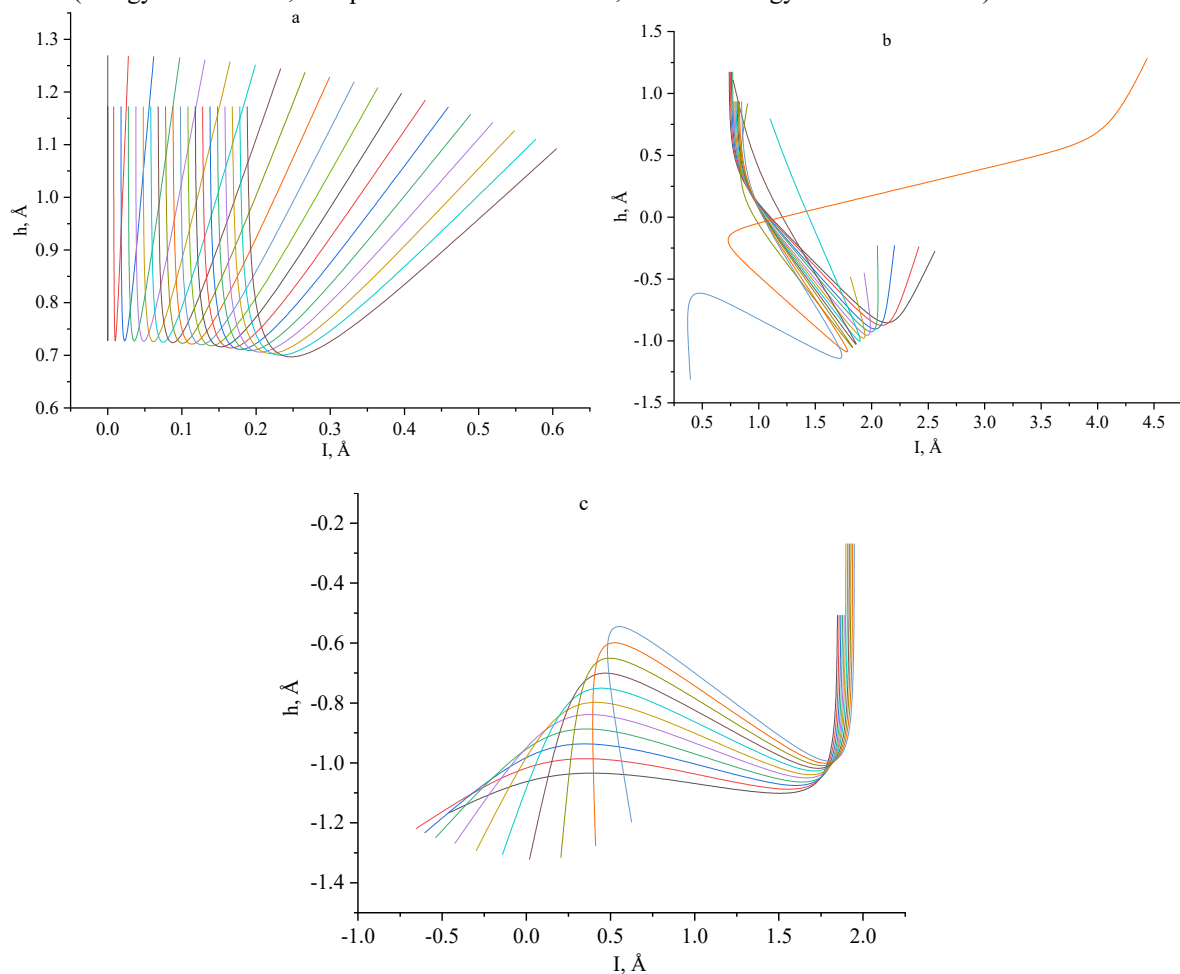


**Figure 3.** Trajectories of scattered ions from the surface atom (a), from the wall of the semichannel (b) and semichannel (c) of the CdTe(001) <110> surface at  $\psi=3^\circ$  and  $E_0=1$  keV

We also simulated the trajectory of  $\text{Ar}^+$  ions scattered from the surface of CdTe(001) <110> at  $\psi = 7^\circ$ , with an initial energy of 1 keV (Fig. 4). It can be seen from the figure that the dense areas have become blurred and their step is equal to 3. This indicates that the changes in the reflected part from the incident one have increased. Note that reflections from

the surface atom and the bottom atom of the semichannel became more accurate. It is also clear that at this sliding angle the number of implanted ions has increased.

In Fig. 5a. the trajectories of scattered ions from a surface atom is presented. It can be seen that the steel trajectories were still moving towards the center of the semichannel than at the incidence angle  $\psi=3^\circ$  and accordingly the energy of the scattered ions decreased to 959 eV, the collision coefficient was equal to 3, and the inelastic energy loss was -7 eV. In Fig. 5b. the trajectories of scattered ions from group 2 are presented. The difference between these trajectories and the case at  $\psi=3^\circ$  is that the upper part narrowed and the lower part became wider. The energy of scattered ions is 935-984 eV, the collision coefficient is 7-12, inelastic energy losses are 15-23 eV. The trajectory of scattered ions from the bottom of the semichannel is shown in Fig. 5c. It can be seen that the ions, scattering from the bottom of the semichannel, were implanted into the crystal. The energy of these ions is -992-995 eV, collision coefficient is 4, inelastic energy losses are 4-6 eV.

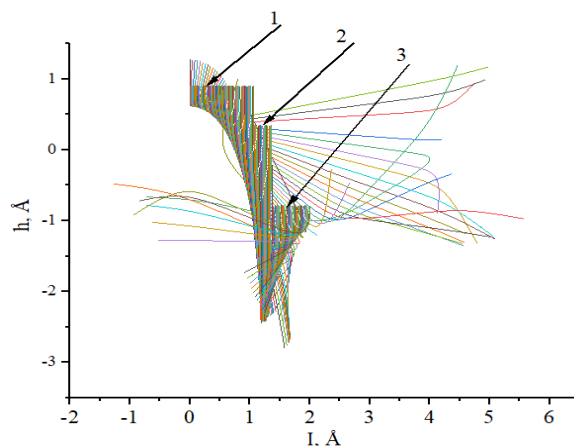


**Figure 4.** Trajectories of scattered ions from the surface of CdTe(001)<110> at  $\psi=7^\circ$  and  $E_0=1$  keV

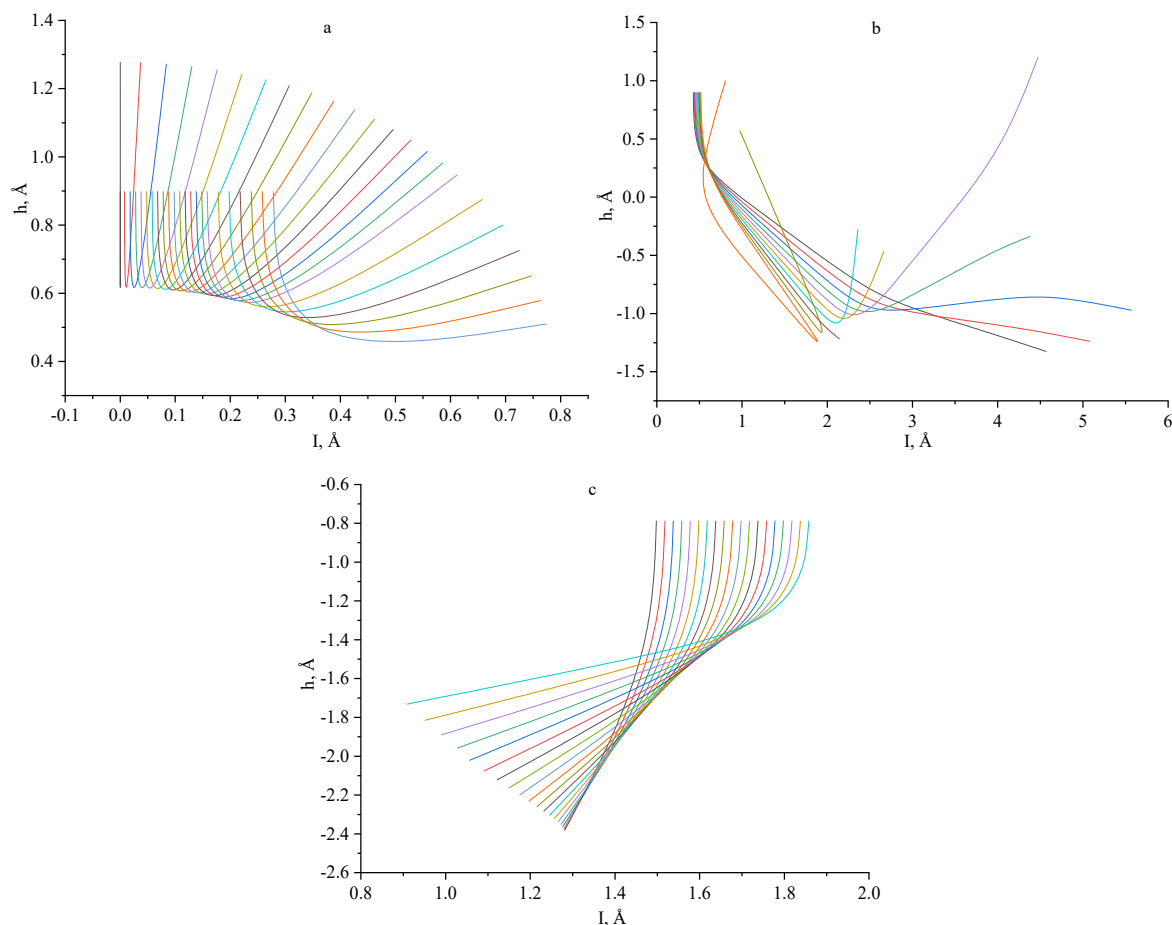


**Figure 5.** Trajectories of scattered ions from the surface atom (a), from the wall of the semichannel (b) and semichannel (c) of the CdTe(001)<110> surface at  $\psi=7^\circ$  and  $E_0=1$  keV

## CONCLUSIONS

Ar<sup>+</sup> ions from the surface semichannel formed on the surface of CdTe(001)<110>. Trajectories were obtained at the angle of incidence  $\psi = 3^\circ$  and  $7^\circ$ , with an initial energy of 1 keV. The influence of increasing the grazing angle on the trajectory of scattered ions is shown. It has been established that an increase in the angle of incidence of bombarding particles leads to a change in the trajectory of scattered ions. With increasing angle of incidence of ions, the Ar<sup>+</sup> part of the trajectory that is located inside the semichannel narrows and therefore it becomes clearer to obtain information about the location of the atoms on the surface and bottom of the semichannel. And the trajectories of scattered ions from the surface atom were not subject to change.

## ORCID

Shuhrat R. Sadullaev, <https://orcid.org/0000-0002-1892-440X>; Uchkun O. Kutliev, <https://orcid.org/0000-0003-2241-2025>

## REFERENCES

- [1] H. Brongersma, M. Draxler, M. Deridder, and P. Bauer, "Surface composition analysis by low-energy ion scattering," *Surf. Sci. Rep.* **62**, 63–109 (2007). <https://doi.org/10.1016/j.surfrep.2006.12.002>
- [2] D.R. Baer, and S. Thevuthasan, "Characterization of Thin Films and Coatings, in: Handbook of Deposition Technologies for Films and Coatings," (Third Edition), Chapter 16, edited by P.M. Martin, (William Andrew Publishing, Boston, 2010). pp. 749–864. <https://doi.org/10.1016/B978-0-8155-2031-3.00016-8>
- [3] T. Grehl, E. Niehuis, and H. H. Brongersma, "Surface Microanalysis by Low-Energy Ion Scattering," *Microscopy Today*, **19**(2), 34–38 (2011). <http://dx.doi.org/10.1017/s1551929511000095>.
- [4] D.N. Bernardo, W.A. Ausserer, Y.C. Ling, and G.H. Morrison, "Secondary ion scattering in dark field ion microscopy," *J. Appl. Phys.* **63**, 5638–5646 (1988). <https://doi.org/10.1063/1.340346>
- [5] F. Samavat, B.V. King, and D.J. O'Connor, "Low energy ion scattering," *Surface Review and Letters*, **14**, 31–41 (2007). <https://doi.org/10.1142/S0218625X07009001>
- [6] C.V. Cushman, P. Br ner, J. Zakel, G.H. Major, B.M. Lunt, N.J. Smith, T. Grehl, and M. R. Linford, "Low energy ion scattering (LEIS). A practical introduction to its theory, instrumentation, and applications," *Anal. Methods*, **8**, 3419 (2016). <https://doi.org/10.1039/C6AY00765A>
- [7] D. Primetzhofer, S.N. Markin, J.I. Juaristi, E. Taglauer, and P. Bauer, "Crystal effects in the neutralization of He<sup>+</sup> ions in the low energy ion scattering regime," *Phys. Rev. Lett.* **100**(21), 213201 (2008). <https://doi.org/10.1103/PhysRevLett.100.213201>
- [8] F. Savamat, B.V. King, and D.J. O'Connor, "Low energy ion scattering," *Surface Review and Letters*, **14**, 31–41 (2007). <https://doi.org/10.1142/S0218625X07009001>
- [9] D.O. Boerma, "Surface physics with low-energy ion scattering," *Nuclear Instruments and Methods in Physics Research Section B: Beam Interactions with Materials and Atoms*, **183**, 73–87 (2001). [http://dx.doi.org/10.1016/S0168-583X\(01\)00311-1](http://dx.doi.org/10.1016/S0168-583X(01)00311-1)
- [10] J.J.C. Geerlings, L.F.Tz. Kwakman, and J. Los, "Local work function effects in the neutralization of alkali ions scattered from cesiated surfaces," *Surface Science*, **184**, 305–318 (1987). [https://doi.org/10.1016/S0039-6028\(87\)80359-X](https://doi.org/10.1016/S0039-6028(87)80359-X)
- [11] R.H. Bergmans, W.J. Huppertz, R.G. van Welzenis, and H.H. Brongersma, "Static low-energy ion scattering," *Nuclear Instruments and Methods in Physics Research Section B: Beam Interactions with Materials and Atoms*, **64**, 584–587 (1992). [http://dx.doi.org/10.1016/0168-583X\(92\)95538-3](http://dx.doi.org/10.1016/0168-583X(92)95538-3)
- [12] Z. Fateen, and I. Azhar, "Indium phosphide nanowires and their applications in optoelectronic devices," in: *2016 Proceedings: Mathematical, Physical and Engineering Sciences*, **472**, 2187 (2016). <https://doi.org/10.1098/rspa.2015.0804>
- [13] M.K. Karimov, U.O. Kutliev, and S.B. Bobojonova, "Investigation of angular spectrum of scattered inert gas ions from the InGaP (001) surface," *Phys. Chem. Solid State*, **22**, 742–745 (2021). <https://doi.org/10.15330/pcss.22.4.742-745>
- [14] U.O. Kutliev, M.U. Otabaev, M.K. Karimov, F.K. Masharipov, and I. Woiciechowski, "Scattering of low-energy Ne<sup>+</sup> ions from the stepped surface of InGaP (001)<110> at the small angles of incidence," *Physics and Chemistry of Solid State*, **24**, 542–548 (2023). <https://doi.org/10.15330/pcss.24.3.542-548>
- [15] J.F. Ziegler, J.P. Biersack, and U. Littmark, *The stopping and range of ions in solids*, (Pergamon Press, NY, 1985)
- [16] L.M. Kishinevsky, *Izv. Acad. Nauk. Fiz.* **26**, 1410 (1962). (in Russian)

ДОСЛІДЖЕННЯ РОЗСПОВАННЯ ІОНІВ Ar<sup>+</sup> ВІД ПОВЕРХНІ CdTe(001) <110> ПРИ КОВЗАЮЧОМУ ПАДІННІ

Ш.Р. Садулласв<sup>а</sup>, У.О. Кутлієв<sup>а</sup>, А.Ю. Саїдова<sup>а</sup>, Г.О. Джуманазаров<sup>а</sup>, Р.Р. Рузметов<sup>б</sup>

<sup>а</sup>Ургенчський державний університет імені Абу Райхана Беруні, факультет фізики,  
вул. Хаміда Олімджана, 14, Ургенч 220100, Узбекистан

<sup>б</sup>Військово-академічний ліцей імені Джалолідіна Мангуберді, Ургенч 220100, Узбекистан

У цій статті наведено результати розсіювання іонів на поверхні тонкої плівки CdTe (001) <110>, отримані за допомогою іонної стріп-спектроскопії. Отримано та проаналізовано траєкторії розсіювання іонів Ar<sup>+</sup> з початковою енергією 1 кеВ і при кутах падіння  $\psi = 3^\circ$  і  $7^\circ$ . Показано, що траєкторії розсіювання іонів від поверхневого ряду атомів, від стінки півканалу і від дна півканалу відрізняються одна від одної. Отримано перші траєкторії розсіювання іонів з поверхневого півканалу, що складається з п'яти атомів Cd і Te, розташованих пошарово в два шари. Обговорюються форми цих трьох типів траєкторій і розраховуються енергії, коефіцієнти розсіювання та непружні втрати енергії розсіювання іонів. Показано, що значення енергії, коефіцієнта розсіювання та непружних втрат енергії розсіювання іонів поверхневими атомними рядами мало відрізняються один від одного. Для іонів, розсіювання від стінки напівканалу та від дна напівканалу, значення цих параметрів лежать в межах діапазону.

**Ключові слова:** комп'ютерне моделювання; розсіювання іонів; півканальний; траєкторія розсіювання іонів